A Comparison of the Thermodynamic Stability and Phase Separation Kinetics of Polymer Blends Containing Cyclic Chains of High Molecular Weight

Maria M. Santore,† Charles C. Han, and Gregory B. McKenna*

National Institute of Standards and Technology, Gaithersburg, Maryland 20899

Received July 22, 1991; Revised Manuscript Received February 26, 1992

ABSTRACT: Two blends of polystyrene (PS, 240K molecular weight) and poly(vinyl methyl ether) (PVME, 171K) were compared, where one blend contained exclusively linear chains and the second contained cyclic PS. The PS/PVME system has been well-studied in the past and is known to exhibit a lower critical solution temperature (LCST) and a critical point near 80% PVME/20% PS when the components exceed 10^5 in molecular weight. The cloud point measurements reported here show that over a broad composition range, the cycle-containing blend phase separates at temperatures ~7 °C above the cloud point temperatures of the exclusively linear blend. The critical composition does not shift appreciably in the cycle-containing blend. Time-resolved light scattering studies were used to probe the phase separation kinetics near the critical composition following temperature jumps into the unstable region. Analysis of the intensity growth via Cahn–Hilliard–Cook theory for early stage spinodal decomposition yielded an apparent mutual diffusion coefficient. When this mutual diffusion coefficient was combined with an estimate for the second derivative of the free energy with respect to composition, it was possible to calculate the mobilities of the cyclic and linear polystyrenes in the PVME. While the diffusion coefficients in the two blends were nearly the same when the systems were compared at identical temperature increments above their respective spinodal temperatures, the PS cycles appeared to be less mobile than their linear analogs in linear PVME matrices. Our data cannot be compared directly with other diffusion and rheological studies of cycles in the literature, but our results appear consistent with some of the published trends.

Introduction

Monocyclic polymers have sparked the interest of the polymer physicist because they present a unique opportunity to test established theories such as reptation. Indeed, the perception that, unlike linear chains, ring polymers cannot reptate (in the classical sense)[1] leads one to ponder the mechanisms of diffusion and viscosity for cyclic samples. Viscosity issues have been examined by Roovers[2,3] and McKenna et al.,[4,5] with the main conclusions that low and moderate molecular weight polystyrene cycles are less viscous than their linear analogs but exhibit a similar power-law dependence on molecular weight. The behavior of high molecular weight cycles is, however, controversial, due to questions about the actual entanglement density of ring melts and the possible viscosity-enhancement effects that occur due to small amounts of linear contaminants.[6]

Forward recoil spectrometry measurements[7] of tracer diffusion add another dimension to the mobility issue for cyclic polymers. Mills et al.[7] found that low molecular weight rings diffuse more readily than their linear analogs through linear matrices, but the diffusion of high molecular weight cycles through linear matrices appears retarded relative to that of the linear analogs. These effects become most noticeable at high linear matrix molecular weights, as expected, and can be best understood if diffusional modes such as ring threading are considered in addition to classical reptation and constraint release.

While dynamic properties such as viscoelasticity and diffusion impact the processability of a blend, its thermodynamic properties limit its ultimate utility, motivating us to consider the equilibrium phase behavior of blends containing rings. The topic of blend stability is especially relevant in light of recent interests in composites and polymer alloys. Classical thermodynamic treatments of polymers developed in the context of linear chains do not directly account for backbone topology and are not easily extended to macrocycles. For instance, the Flory χ parameter[8] is defined in terms of the enthalpic interactions between individual segments, and the original definition implies that χ should be independent of molecular weight and composition, which is not in reality the case.[9] One would therefore expect that in addition to composition and molecular weight, molecular architecture will also impact χ.

In this work, we consider the PS/PVME (polystyrene/poly(vinyl methyl ether)) blend where the PS component is macrocyclic. Previous work[10] with the linear PS/linear PVME blend revealed its LCST (lower critical solution temperature) behavior, i.e., phase separation on heating. The fact that this mixture can be thermally destabilized presents the additional opportunity to probe the mutual diffusion coefficient[11] which reflects the interplay between thermodynamics and mobility, the latter of which should directly reflect backbone topology. The mutual diffusion coefficient, extracted via a Cahn–Hilliard–Cook analysis of spinodal decomposition kinetics at short times after the initiation of phase separation, reflects dynamic properties similar to those in previous viscoelastic[2-6] and tracer diffusion[7] studies of high molecular weight cycles, though a direct comparison cannot be made.

Experimental Procedure

In this study we employed two polystyrene (PS) samples. The cyclic sample of molecular weight 247K was synthesized by Hotstetter and Fetters.[5] This sample was determined to be cyclic based on intrinsic viscosity[5] and sedimentation behavior.[12] It was studied by McKenna et al.[5] and was referred to as "82R" in their 1989 rheological characterization paper. Its recoverable creep compliance exhibited a high steady-state value and low shoulder region, indicative of a small amount of high molecular weight contaminants which was thought to be cyclic. The presence of these high molecular weight contaminants is mentioned at this point because of the possibility that they influenced

† Current address: Department of Chemical Engineering, Lehigh University, 111 Research Drive Bldg. A, Bethlehem, PA 18015.

the results presented here. We feel, however, that it is unlikely that small amounts of linear contaminant, within the 82R sample, would significantly affect the blend stability and diffusion results presented in what follows. The θ-temperature for the cyclic sample in cyclohexane was 32.4 °C while a linear PS of molecular weight 240K ("82L" in ref 15) had a θ-temperature of 34.4 °C.[5] Our linear PS, of molecular weight 237K and polydispersity 1.13 (as determined by light scattering), was synthesized by the Strasbourg group.[13] It too had been studied previously, and in the McKenna publication was referred to as "HA52". These polystyrenes were used in two blends with a poly(vinyl methyl ether) of molecular weight 171K and polydispersity 1.42 (as determined by chromatography), synthesized at the National Institutes of Standards and Technology. A small amount (0.05 wt %) of Santonox R[21] was added to each blend to prevent oxidation during heating.

Blends were cast from toluene solutions onto microscope slides for cloud point tests and onto quartz windows for light scattering. Samples were first air-dried on a hot plate at 60 °C for several hours and then kept in a vacuum oven at 75 °C for several days prior to the addition of cover-slips or top windows. Before testing, samples were stored in the dark under vacuum in a desiccator with P_2O_5.

Cloud point tests at heating rates of 0.1 °C/min determined the phase separation temperature as a function of composition. Near the critical composition, a temperature change moves the system from a stable to an unstable region, so that the measured phase separation temperature is indicative of both the spinodal and binodal lines. At noncritical compositions, a temperature increase brings the system through a metastable region into an unstable region. Phase separation may not occur immediately in a metastable zone, hence at noncritical compositions, the measured cloud point temperature may lie between the spinodal and binodal curves. We have treated these data as the binodal temperature for slow heating rates.

Time-resolved light scattering, described in detail in a previous publication,[14] was carried out near the critical composition of 20% PS/80% PVME, as determined by our cloud point curves. Samples were preheated for approximately 1 h at 105 °C, a temperature significantly below the anticipated spinodal. Moving the sample from the preheating block to light scattering block (at the final temperature) accomplished the rapid temperature jump. Final temperatures were chosen in the range of the anticipated spinodal temperature, up to 2 °C into the two-phase region. With thermal equilibration times less than 1 min, data acquisition commenced 1 min after the temperature jump. An array detector measured intensity as a function of time over a range $q = (4\pi/\lambda) \sin(\theta/2)$ from 5 to 20 μm^{-1}. Data collection slowed with time in anticipation of an exponential-like dependence of scattering on time.

Analysis of the Time-Resolved Light Scattering Data. The analysis of the time-resolved light scattering experiments via Cahn–Hilliard–Cook theory has been presented by Sato and Han[14] and is summarized here for completeness. Following a temperature change, the evolution of the structure factor $S(q)$ is governed by a complicated differential equation. However, if concentration fluctuations are small at short times after the quench, an average composition, Φ_0, can be used for an approximate solution that neglects higher orders in S_n:

$$S(q,t) = S_\infty + (S_0 - S_\infty)e^{2R(q)t} \tag{1}$$

with

$$R(q) = -Mq^2\left(\frac{\partial^2 f}{\partial \Phi_0^2} + 2\kappa q^2\right) \tag{2}$$

Here S_∞ is the virtual structure factor arising from thermal noise and S_0 is the intensity at time $t = 0$. The appearance of Φ_0 in the second derivative of the free energy, f, with respect to composition reflects the linear approximation. In the early stage of spinodal decomposition, the phase separation follows exponential growth (if thermal fluctuations contribute negligibly) such that R depends only on the scattering vector. The mobility, M, for polymer blends generally depends on q but can be treated as a constant if $q < R_g^{-1}$. Finally, κ accounts for interfacial effects and depends on Φ_0 and system parameters.

Equation 2 can be rewritten in a form that includes the inter (or mutual) diffusion coefficient D

$$R(q) = -Dq^2 - 2M\kappa q^4 \tag{3}$$

such that $D = M(\partial^2 f/\partial \Phi^2)$. While M reflects system-specific properties such as molecular architecture, the diffusion coefficient is additionally complicated by thermodynamic effects. The second derivative of the free energy reflects the stability of the system, decreasing from positive to negative values as the system becomes unstable. Both $\partial^2 f/\partial \Phi^2$ and D vanish at the limit of stability. Since we measure the mutual diffusion coefficient during a phase separation process, we anticipate negative diffusion coefficients which are not an unphysical result, but a mere reflection of the instability.

Traditionally, $R(q)$ has been determined by plotting log $I(q)$ or log $S(q)$ against t;[11] however, this type of analysis requires the background intensity and virtual structure factor which were often ignored or assumed negligible. In reality, these terms may be significant, motivating our use of a "$^1/_3$ plot",[14] in which $\{t/[I(t) - I(t=0)]\}^{1/3}$ is shown as a function of t, as an alternative to the logarithmic analysis. The expression derives from the intensity $I(q,t)$ during the early stage of phase separation:

$$I(q,t) = KS_\infty + I_b + K(S_0 - S_\infty)e^{2R(q)t} \tag{4a}$$

$$= I_\infty + (I_0 - I_\infty)e^{2R(q)t} \tag{4b}$$

where the background intensity, I_b, is included in both

$$I_\infty \equiv KS_\infty + I_b \tag{5a}$$

and

$$I_0 \equiv KS_0 + I_b \tag{5b}$$

Expanding for $R(q)t < 1$ and rearranging yields

$$\left[\frac{t}{I(qt) - I_0}\right]^{1/3} = \frac{1}{[2(I_0 - I_\infty)R(q)]^{1/3}}\{1 - {}^1/_3R(q)t + 0(t^3)\} \tag{6}$$

Equation 6 does not include a second-order term t^2 and thus may be truncated at the $^1/_3R(q)t$ term. Further, using 6 should be preferable to an analysis that employs eq 4b since the former avoids the complication of background scattering and the virtual structure factor. Sato and Han[14] have compared both types of analysis and found the "$^1/_3$ plot" method superior since the resulting calculated $R(q)$ more nearly obeys $R(q)/q^2$ vs q^2 over a large q range. However, the "$^1/_3$ plot" is an interactive analysis with time on both axes and can easily be confounded by scatter in the data.

In this study, we employed both logarithmic and "$^1/_3$ plot" analysis methods to determine $R(q)$. The mutual diffusion coefficient was determined from a plot of $R(q)/q^2$ against q^2. Finally, thermodynamic and mobility contributions to the diffusion coefficient were estimated, assuming literature[14] values for the second derivative of the free energy with respect to average composition.

Results

Figure 1 presents cloud point phase diagrams for PS/PVME blends over the composition range from 10 to 65 wt % PS for both the cyclic and linear polystyrenes. In this figure, the two-phase region for each blend lies above its curve. On both curves, the critical point is near the composition 20% PS/80% PVME; however, the entire phase envelope is shifted 7–8 °C higher when the polystyrene is cyclic. Over a temperature range of 7–8 °C, the blend which contains cyclic PS is stable but the blend of exclusively linear components is unstable.

Figure 2 shows the evolution of intensity with time at several q values following a rapid temperature jump into the two-phase region, approximately 1 °C above the spinodal (the determination of the exact spinodal is shown

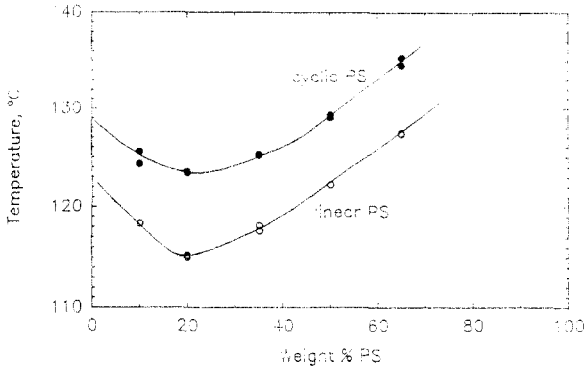

Figure 1. Cloud point curves for blends of cyclic and linear PS (240K) with linear PVME (171K). The area above each curve is the two-phase region for that system.

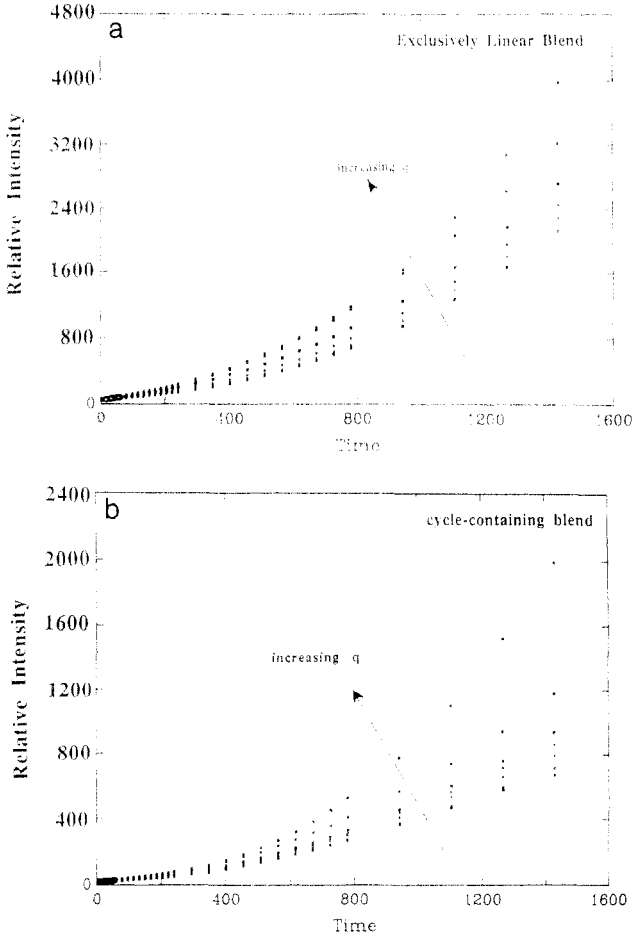

Figure 2. Raw scattering data from PS/PVME blends undergoing phase separation: Intensity as a function of time in seconds for several values of q: 5.76, 7.24, 8.47, 9.46, 10.49, 11.49, 12.63 μm^{-1}. (a) Blend containing linear PS, temperature = 116 °C. (b) Blend containing cyclic PS, temperature = 122 °C.

later) for the two systems. There is a qualitative similarity between the raw data in Figure 2a where the blend contains exclusively linear components, and Figure 2b where the PS is cyclic. The scale of the vertical axis reflects background scattering, and the values at time zero correspond to the scattering 1 min after the temperature jump. Also note that the $I(t)$ curves for the largest and smallest q values are slightly out of step with the rest of the data. We attribute this anomaly to the array detector, which in its current configuration tends to magnify the signal from either end of the diode array.

Figure 3 shows the data from Figure 2 presented as log $I(q)$ vs t. Even for short times, the $I(t)$ trace for a given q has significant curvature, indicating that eq 3 is not

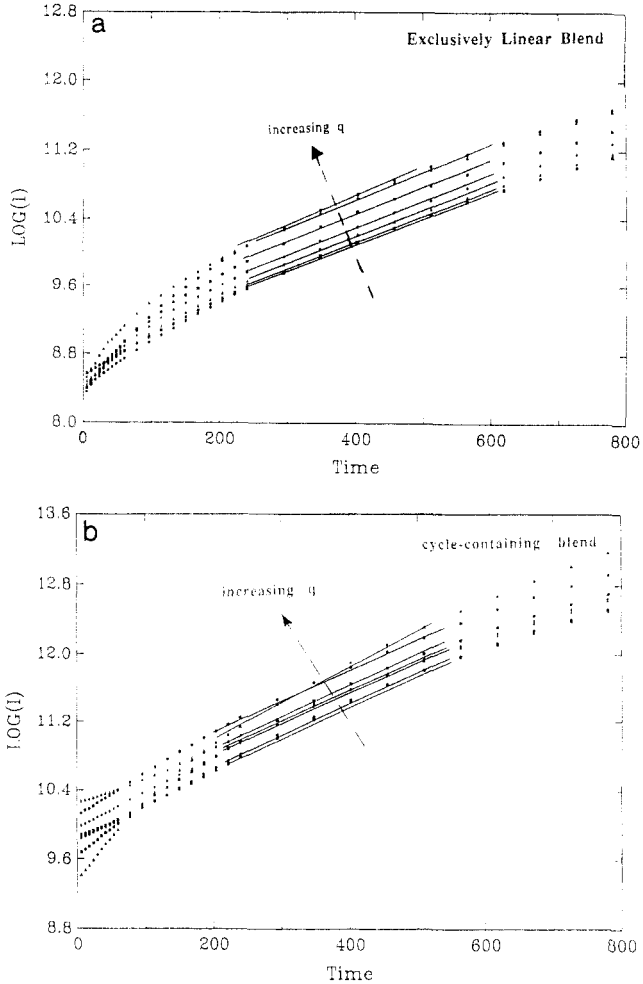

Figure 3. Semilog plot of intensity vs time in seconds for the data in Figure 2. (a) Blend containing linear PS, temperature = 116 °C. (b) Blend containing cyclic PS, temperature = 122 °C.

exact, either because of contributions from background scattering for thermal fluctuations, or because the nonlinear effects, approximations made in deriving eq 1, are more important than anticipated. We have drawn lines through this data to indicate our interpretation of $R(q)$ according to eq 4b and to illustrate the q range over which we apply eq 4. Rather arbitrarily, the analysis is restricted to times less than 800 s for the early stage of spinodal decomposition. Indeed, the ultimate values of $R(q)$ from this analysis satisfy the requirement $tR(q) < 1$. Within the first 800 s, we have experimented with the analysis, applying it to subsets of the data, for instance, 100–300 s, 300–500 s, etc. This variation due to the "time frame" of the data analysis is represented as error bars in later plots.

Figure 4 shows the "$^1/_3$ plot" analysis of the data from Figure 2. As in Figure 3, these curves are also not perfectly linear, and again we limited our linearization to short times: 800 s or less after the temperature change. The lines indicate our interpretation of the appropriate slope and intercepts. The evolution of the scattering function is qualitatively similar in the cases of exclusively linear and cycle-containing blends, although actual values depend on the background scattering of a particular sample.

Parts a and b of Figure 5 show $R(q)/q^2$ at selected temperatures for PS/PVME blends containing linear and cyclic PS, respectively. We determine D_{app} from the intercept according to eq 3. This analysis is preferred over a $R(q)$ vs q^2 plot because the q^4 term is apparently important in our systems. Note, however, that eq 3 specifies a linear function for Figure 5 and our data exhibit curvature. The

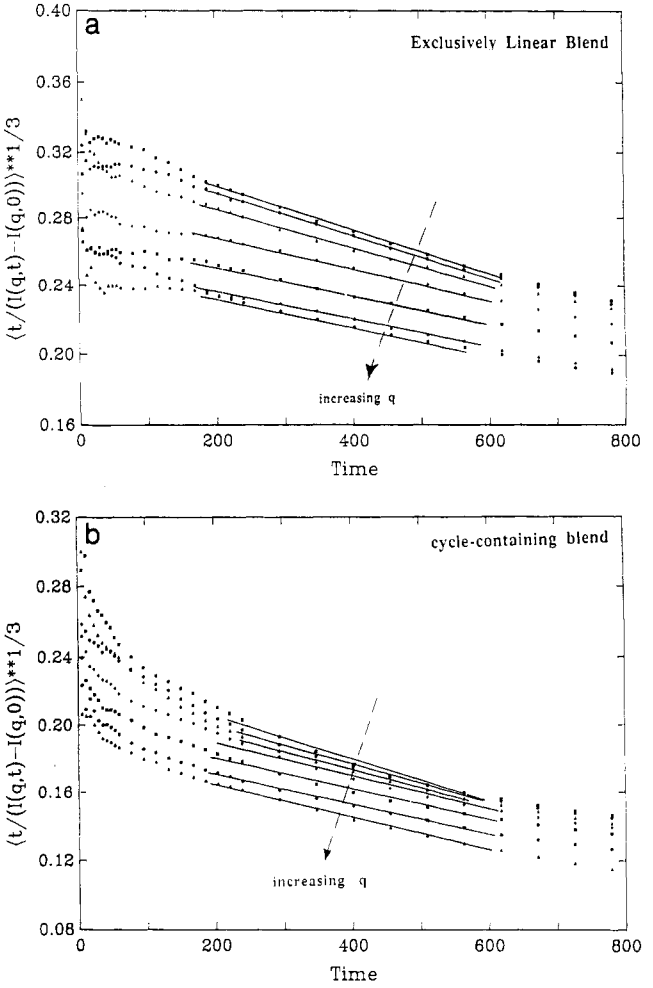

Figure 4. "$^1/_3$ plot" analysis of data from Figure 2. (a) Blend containing linear PS, temperature = 116 °C. (b) Blend containing cyclic PS, temperature = 122 °C.

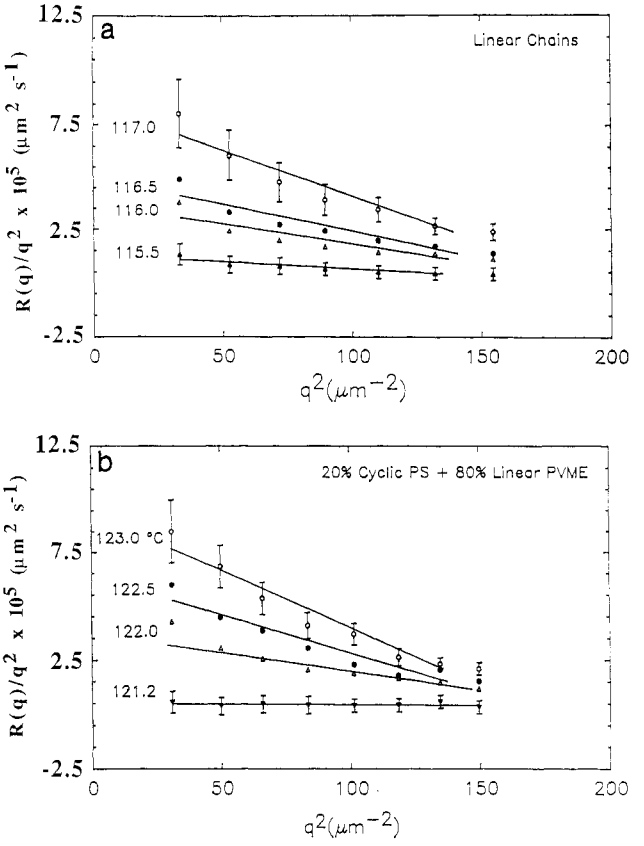

Figure 5. $R(q)/q^2$ vs q^2 at several temperatures. Extrapolation to q = 0 yields the mutual diffusion coefficient. (a) Blend containing linear PS, temperature = 116 °C. (b) Blend containing cyclic PS, temperature = 122 °C.

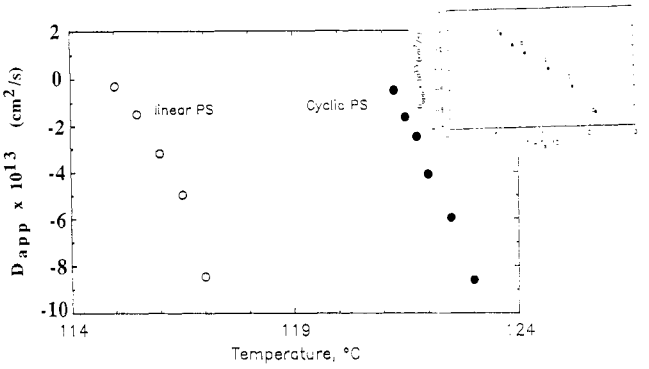

Figure 6. Apparent mutual diffusion coefficients (at 20% PS/80% PVME) as a function of temperature for blends containing linear and cyclic PS.

error bars on the data taken at the highest and lowest temperatures of each plot indicate the range for $R(q)$ that can be calculated from a $^1/_3$ plot analysis using a least squares fit for different data subsets: 100–300 s, 300–500 s, 500–800 s, and 0–800 s. (Points derive from the "fit by eye" technique of Figures 3 and 4.) Note that the variation in R with the arbitrary choice of data subset (or "time frame") shows the greatest dependence on this choice of data when temperatures are deep in the two-phase region and q is small. Note also that the qualitative similarity between blends with exclusively linear components and those with cyclic PS in Figures 3 and 4 leads to a similarity between the two systems when $R(q)/q^2$ is plotted as a function of q^2 in Figure 5. The raw intensity in Figure 2 is not quantitatively reproducible at constant composition from one sample to the next; however, the background scattering and virtual structure factor fall out in the $^1/_3$ plot analysis, as does I_0 in the logarithmic analysis, to yield $R(q)$ behavior that is reproducible from one sample to the next.

Figure 6 summarizes the diffusion coefficients as functions of temperature for both blends. These values are negative because the system is unstable, and each species diffuses against its gradient as the system phase separates. The second derivative of the free energy vanishes at the limit of stability (i.e. phase separation temperature) and so must the diffusion coefficient. This fact enables us to extrapolate spinodal temperatures T_s = 114.9 °C for the exclusively linear blend and T_2 = 121.1 °C for the blend containing cyclic PS. Interestingly, as shown in the inset, the apparent mutual diffusion coefficients for the rings and linear polystyrenes are the same within experimental error when the results are compared at equal temperature increments above the relevant spinodal temperatures. We discuss the mobility in the next section.

Discussion

Static Properties. The cloud point studies indicate that the cyclization of the PS component tends to stabilize the PS/PVME mixture over a broad composition range. Of course, the temperature where the mixture becomes turbid depends on the relative rates of the phase separation and the temperature change. Faster heating rates will yield higher cloud points. We have used a slow heating rate of 0.1 °C/min to obtain the data in Figure 1. If, in reality, the phase separation temperatures of the two systems were identical, a significant difference in their separation kinetics would be needed to explain the elevated cloud point of the blend containing cyclic PS. The time-

resolved light scatering studies, however, show that there is a true difference in the spinodal temperatures. We do not expect this stabilizing trend to result from the cycle-closing chemical group since the molecular weight of our PS is relatively high. Also, McKenna and co-worker's[5] rheological characterization of our cycles indicates small amounts of high molecular weight cyclic impurities. Such high molecular weight contaminants might be expected to diminish the stabilizing effect. If so, with purer cyclic PS, we would observe even greater temperature differences in the two-phase envelopes in Figure 1.

The stability results in Figure 1 are not predicted by any theory of which we are aware, but are consistent with Cates and Deutch's expectation[15] of a negative χ parameter for rings mixed with chemically identical linear chains, evidenced by the predicted swelling of cycles in linear matrices.[16,17] An extension[15] of this logic suggests that there might exist pairs of immiscible linear polymers that become miscible when one component is cyclized prior to blending.

Our observations, that PS/PVME blends employing cyclic PS are more compatible than those with linear PS, also seem consistent with the observation of a depressed θ-temperature in solutions of polymer cycles.[5,18] A lower θ-temperature favors solubility, i.e. the solution is made more stable at a given temperature by the cyclization of the solute. This point can also be argued in terms of the changes that cyclization induces in the free energy of one pure component of a solution or blend.

Kinetics and Diffusion. The analysis of phase separation kinetics to extract the mutual diffusion coefficient is complicated by thermal fluctuations and the inherent nonlinearities of the phase separation process. Indeed, the linear Cahn–Hilliard–Cook theory restricts us to the early stage of phase separation kinetics. Further, Sato and Han[14] derive the expansion for the $^1/_3$ plot analysis explicitly for $R(q)t < 1$. Values for $R(q)$ on the order of 10^{-3} s^{-1} restrict our analysis to times less than 10^3 s. Note, however, for $T - T_s > 0$ at small q, R increases with q such that different time limitations apply at different q values. Deeper in the unstable region, phase separation occurs more rapidly, so that analysis must also be restricted to shorter time frames as $T - T_s$ is increased. We have observed that for shallow quenches, $0 < T - T_s < 0.5$ °C, the phase separation kinetics follow near exponential growth. Deviations from exponential growth increase with temperature. This is manifest on the $R(q)/q^2$ vs q^2 plots, where the data near T_s are most nearly linear, but curvature increases as $T - T_s$ grows.

It is worth mentioning that in their studies of the PS/PVME blend, Hashimoto et al.,[11] who invoke the logarithmic analysis to obtain $R(q)$, also observe apparent nonlinearities in their intensity and $R(q)/q^2$ plots. Sato and Han[14] present some of the cleanest data, where not only is $R(q)/q^2$ linear in q^2, but the q^4 term is negligible, facilitating plots of $R(q)$ vs q^2. They attribute the good quality of their data to the $^1/_3$ plot method, and provide a very convincing comparison between "$^1/_3$ plot" and logarithmic analysis methods that favors the former. A close scrutinization, however, of their $^1/_3$ plots also reveals curvature. Perhaps a different hand choosing the best linear fit would have introduced more curvature into Sato and Han's[14] $R(q)$ vs q^2 figure or removed some of the curvature from our Figure 5.

Our concern about the objectivity of the method and time range (i.e. 0–800 s vs 300–500 s) for the analysis led us to use both logarithmic and $^1/_3$ plot methods; however, $R(q)$ values obtained by the logarithmic analysis fell within the error bars in Figure 5. This suggests that the virtual structure factor does not make significant contributions to overall scattering in our experiments. Nonlinearities must then result from thermal fluctuations or the intrinsic kinetics, with both mechanisms becoming more important as $T - T_s$ is increased.

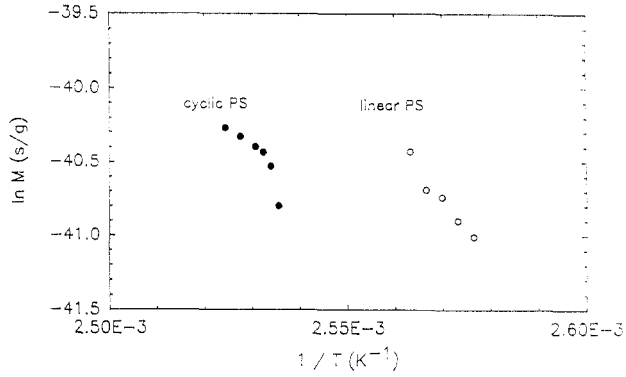

Figure 7. Arrhenius plot for mutual mobilities at 20% PS/80% PVME comparing the cycle-containing blend to that of exclusively linear components.

Stephenson[19] has considered deviations from the Cahn–Hilliard theory in the spinodal decomposition of glasses by introducing a diffusion-induced flow model. This motivated us to explore the possibility of relaxational contributions to our kinetics and also fit data to a stretched exponential, typical of many relaxation processes. Discussion of this analysis is included only as an appendix since it did not simplify our interpretation of the kinetics, but suggested that relaxation processes do not dominate the kinetics for our system. The stretched exponential analysis, however, provides an interesting measure of the "nonlinearity" of the phase separation kinetics and as such perhaps deserves further exploration in the future.

In Figure 6, the insensitivity of the apparent diffusion coefficient to molecular architecture was unexpected. Our diffusion coefficient values are approximately 3 times higher than those reported by Sato and Han,[14] when compared at constant $T - T_s$. (This effect is manifested by the different slopes of the data in Figure 6 and the respective plot in the Sato and Han[14] paper.) This is a consistent result since their components were almost twice as high in molecular weight as the respective components in our experiments, and their phase separations occurred at significantly higher temperatures (by almost 30 °C). In Figure 6, the effects of molecular architecture on chain motion may be hidden by thermodynamic contributions to the diffusion coefficients. Additionally, the vanishing of $d^2f/d\Phi^2$ at the spinodal requires that D become zero for both linear blends and those containing cycles at their respective spinodal temperatures. In order to examine the true transport behavior of the two blends, i.e., to calculate the mobility (see eq 3), we invoke Sato and Han's empirical expression[14] for $d^2f/d\Phi^2$ (T, T_s) which applies to several molecular weight combinations of the deuterated PS/protonated PVME system:

$$\frac{\partial^2 f}{\partial \Phi^2} = (2.18 \times 10^9)(1/T - 1/T_s)\ \text{J m}^{-3} \qquad (7)$$

This relationship may not apply exactly for our PS/PVME system, due to our cyclization of the PS and their deuteration of the PS. By employing eq 7, we determined mobility as a function of temperature. The results are presented as ln M vs $1/T$ in Figure 7. (Note that the temperature range studied of 2 °C is too small to distinguish between Arrhenius and Vogel or WLF types of temper-

ature dependence.) Here, the linear chains are significantly more mobile than their cyclic analogs at the same temperature. To see this one must either extrapolate the data for the cycle-containing to lower temperatures, or that for the exclusively linear blend to higher temperatures. In previous experiments, Sato and Han[14] show that the Arrhenius representation is reasonable since $dM/d(1/T)$ is nearly constant across the spinodal for a total temperature range of almost 10 °C. The temperature range of Figure 7 is too narrow for a precise extrapolation; however, even with a broad range of possible $dM/d(1T)$ values it is clear that the cycles are less mobile in the blend. We note further that the most reliable data in Figure 7 are those points furthest from the spinodal for each system. As $T \rightarrow T_s$, $\partial^2 f/\partial\Phi^2$ becomes vanishingly small, magnifying errors in D when M is calculated.

We emphasize that the two assumptions needed to arrive at Figure 7 were (1) that the dependence of $\partial^2 f/\partial\Phi^2$ is the same for protonated and deuterated PS mixed with PVME and (2) that cyclization does not appreciably affect $\partial^2 f/\partial\Phi^2$. At this stage, we have no gauge of how appropriate these approximations are, and SANS (small angle neutron scattering) work is underway to estimate the values of $\partial^2 f/\partial\Phi^2$ required for a more precise calculation of $M(T)$ for our two blends.

Even given the possible errors in Figure 7, the observation of a reduced mobility for cycles is very interesting: One interpretation is that cycles have a lower mobility in linear matrices than do the linear chains themselves in a linear matrix. An alternate interpretation, though, is that the addition of cyclic molecules decreases the mutual mobility of linear chains in a mixture, even when cycles comprise a fraction (20%) of the total polymer mass. This latter interpretation complements rheological data, i.e. McKenna and Plazek's[6] observation that addition of linear contaminants drastically increases the viscosity of cyclic PS samples. The apparent immobilization effect then appears for cycles added to linear matrices and vice versa. As noted earlier, there remains the possibility that contaminants from the 82R cycles have affected these mobility results. This may initially appear to be a reasonable conclusion since linear contaminants have been shown to dramatically impact the viscosity of a cyclic sample. We remind the reader, however, that the results presented here approach another case where high molecular weight species, especially linear contaminants in 82R, would be expected to have less of an effect. It must be emphasized that the cycles here are mixed with PVME to yield a blend whose ultimate linear content is near 80%. Any contaminants from the PS should therefore have less of an effect then those deliberately added in McKenna and co-worker's[5,6] rheological investigations.

One issue that must be addressed is the possibility that the temperature jump experiments were not performed exactly at the critical composition of each blend. Since cloud point tests were run at intervals of 10% or 15% PS, we have not proven that the critical compositions of the two blends are exactly the same. We are fairly certain of the critical composition of 20% PS/80% PVME in the exclusively linear blend, since this value agrees with previous work.[10,11,14] The critical composition in the cycle-containing blend is less certain only because it has not been reproduced by other groups. A significant shift in the critical composition in the cycle-containing blend seems contrary to the consistently higher cloud points in Figure 1. Indeed, the uniformity of the temperature shift (6–7 °C) argues against a significant error in our reported critical composition in this mixture.

A second important issue is the effect of temperature relative to the glass transition of each system. While eq 7 corrects for the temperature effect near the spinodal, enabling mobility calculations, the effect of T_g remains unresolved. We note first, that for rings of high molecular weights such as ours, cyclization is expected to have negligible effects on T_g,[20] and this has been confirmed for PS cycles.[3-5] Though we have not run DSC tests on our samples, we expect nearly identical T_g's for the two 20% PS/80% PVME systems, definitely below room temperature, and probably near 0 °C. Our tests are run, therefore, over 110 °C above the T_g for the two blends. (During the time frame to which the Cahn–Hilliard–Cook analysis is applied, phase separation is underway; however, the bulk of the polymer molecules are in "interfacial regions" where the composition varies spatially. The two equilibrium compositions have not been realized; therefore, the chances of having regions of pure PS and pure PVME due to fluctuation are remote. We therefore do not concern ourselves with the fact that a pure PS phase in our experiments would exist 10–20 °C above its T_g.) The question is, then, whether the 7 °C difference in the temperature range of the two temperature jump studies will significantly impact the dynamic properties of the molecules. The cycle-containing blend phase separates at the higher temperature and should, if cyclization were to have no effect, separate more rapidly. In other words, the hotter system should exhibit greater mobility since it is further removed from T_g. We observe, however, that the cycle-containing blend exhibits a lower mobility, contrary to the expectation from the T_g argument. Hence, if we were to correlate the mobilities of Figure 7 against $1/(T - T_g)$ rather than $1/T$, we would observe an even greater difference in the mutual mobilities of the two blends.

Because our experiments measure an apparent mutual diffusion coefficient for two chemical species in the sense that the system is well-mixed only in the limit $t \rightarrow 0$, and Mills'[7] experiments yield a tracer diffusion coefficient for cyclic PS in a linear PS matrix only as $t \rightarrow \infty$, a direct comparison between the two studies is impossible. It is an interesting coincidence, however, that both studies yield diffusion coefficients on the order of 10^{-14} cm^2 s^{-1}. Even more important, however, is that Mills et al.[7] observe a significant difference between the highest molecular weight (180K) cycles and the linear analogs diffusing through a linear matrix. With linear matrices below molecular weights on the order 10^5, cycles diffuse up to 3 times faster than their linear analogs. Just above matrix molecular weights of 10^5, the diffusion coefficient for large cycles approaches that for linear chains, and at higher molecular weights, rings diffuse up to 1.5 orders of magnitude more slowly than their linear analogs. From these studies, we estimate that for linear matrices on the order of M_w = 170 000, the cyclic diffusion coefficients would be half those of the analogous linear chains. This observation is consistent with our observations, but direct comparisons are confounded by the extreme differences in the two systems.

Conclusions

We have compared the LCST phase envelopes of two PS/PVME blends: one with exclusively linear components and a second containing cyclic PS, each component having a molecular weight greater than the entanglement molecular weight of the pure component. The blend containing the cyclic PS yielded a cloud point curve that was elevated 7–8 °C above that for the exclusively linear blend, at compositions from 10% to 65% PS. Furthermore, cy-

Table AI
Summary of Fits for Phase Separation at 116 °C of Exclusively Linear Blend

		stretched exponential fit				exponential fit		
q (μm^{-1})	time frame (s)	I_0	R (s^{-1})	α	χ^2	I_0	R (s^{-1})	χ^2
25	0–800	3500	0.0036	0.63	2.8×10^6	6600	0.0015	1.0×10^8
	0–100	4200	0.0026	0.80	1200	4500	0.0028	43000
	300–500	3200	0.0040	0.62	2300	5700	0.0018	1.0×10^6
	500–800	1900	0.0087	0.49	1.1×10^5	9600	0.0013	1.9×10^6
38	0–800	3500	0.0049	0.56	8.1×10^5	7900	0.0015	1.0×10^8
	0–100	4200	0.0037	0.80	17000	4600	0.0036	1.0×10^5
	300–500	4000	0.039	0.62	42000	7000	0.0018	1.4×10^6
	300–800	3400	0.0052	0.55	1.4×10^5	11800	0.0012	2.0×10^6
53	0–800	1700	0.022	0.41	5.5×10^6	10000	0.0016	7.4×10^8
	0–100	3700	0.0052	0.73	30000	4300	0.0046	2.7×10^5
	300–500	900	0.073	0.33	1.2×10^5	8000	0.0021	1.1×10^7
	500–800	1400	0.031	0.38	4.3×10^5	17000	0.0012	6.6×10^6

Table AII
Summary of Fits for Phase Separation at 122 °C of Cycle-Containing Blend

		stretched exponential fit				exponential fit		
q (μm^{-1})	time frame (s)	I_0	R (s^{-1})	α	χ^2	I_0	R (s^{-1})	χ^2
25	0–800	13000	0.0035	0.66	2.3×10^8	24000	0.0016	1.5×10^9
	0–100	19000	0.0021	1.12	18000	18000	0.0019	1.0×10^5
	100–400	14000	0.0029	0.78	34000	19000	0.0020	5.1×10^6
	400–800	5700	0.0107	0.48	2.1×10^7	35000	0.0013	9.5×10^7
38	0–800	15000	0.0033	0.67	2.7×10^8	27000	0.0016	1.8×10^9
	0–100	21000	0.0022	1.07	31000	21000	0.0021	78000
	100–400	19000	0.023	0.88	9.2×10^5	22000	0.0020	2.6×10^6
	400–800	7400	0.0092	0.50	1.5×10^7	40000	0.0013	9.4×10^7
53	0–800	17000	0.0040	0.63	2.6×10^8	35000	0.0016	3.6×10^9
	0–100	24000	0.0026	1.06	80000	24000	0.0025	1.6×10^5
	100–400	17000	0.0037	0.67	7.8×10^5	29000	0.0020	2.5×10^7
	400–800	8600	0.010	0.48	4.9×10^7	52000	0.0013	2.1×10^8

clization does not appear to shift the critical composition significantly, though more tests are needed to establish this with certainty.

Time-resolved light scattering studies of the phase separation kinetics yield mutual diffusion coefficients when data analysis is based on Cahn–Hilliard–Cook theory for the early stage of spinodal decomposition. The mutual diffusion coefficients near the critical composition (20% PS/80% PVME) of the two systems are nearly identical when comparisons are made at the same temperature increments above the respective spinodal temperatures. An estimate of the second derivative of the free energy makes possible the calculation of the mobilities at various temperatures. Here it is apparent that molecules within the cycle-containing blend are significantly less mobile than those in the exclusively linear blend. This is true even though the cycle-containing blend was measured 7 °C higher above its T_g compared to the exclusively linear blend.

Direct comparison with literature on cycles is not possible; however, our static and dynamic results are consistent with prior work. For example, the stability enhancement of a few degrees by the cyclization of one blend component complements the observation of a depressed θ-temperature for solutions of cycles with respect to their linear analogs. The stabilizing effect is also consistent with ring threading and the expansion of rings in linear melts predicted by computer simulations. The link between ring expansion and enhanced stability can be rationalized in terms of a negative χ parameter for blends of rings and linear chains of the same chemical makeup and by an increased energy of the pure cyclic melt.

Our mobility results are consistent with the data of Mills et al.[7] for diffusion of cycles through chemically identical linear matrices. More important, though, is that our observation of slower cyclic mobility relative to linear chains in linear matrices concurs with the observation that linear contaminants drastically increase the viscosity of cyclic melts.[5,6]

Acknowledgment. This project was funded by a NRC postdoctoral fellowship to M.M.S. We would like to thank Dr. B. Bauer for his generous gift of the PVME, Dr. R. Briber for his insight into the equilibrium effects of cycle-containing blends, Mr. Yi Feng for his help in overcoming experimental complications and ambiguities in the data analysis, and Dr. J. Douglas for stimulating discussions on relaxation processes. We also wish to thank P. Lutz, G. Hild, and P. Rempp of the Institut Charles Sadron, Strasbourg, for the linear polystyrene as well as L. J. Fetters of Exxon and B. J. Hotstetter of Hercules, Inc., for the cyclic polystyrene.

Appendix

Since stretched exponential time dependencies are typical of relaxations in glasses and in polymer melts, we attempted to fit the intensity growth to the following form, where the parameters I_0, $R(q)$, and $\alpha(q)$ were chosen to minimize the square error:

$$I(q,t) = I_0(q) \exp[2R(q)t]^{\alpha(q)} \quad \text{(A1)}$$

The fit was performed for each phase separation run at several q values from 5 to 20 μm^{-1}; however, not all of these are shown, because the quantity of information is overwhelming. For comparison, we also fit the data to the standard exponential form for each chosen q value:

$$I(q,t) = I_0(q) \exp[2R(q)t] \quad \text{(A2)}$$

Here only two parameters, I_0 and $R(q)$, are determined in the analysis.

Figure 8 shows two examples of phase separation kinetics at three values of q for (a) the exclusively linear blend and

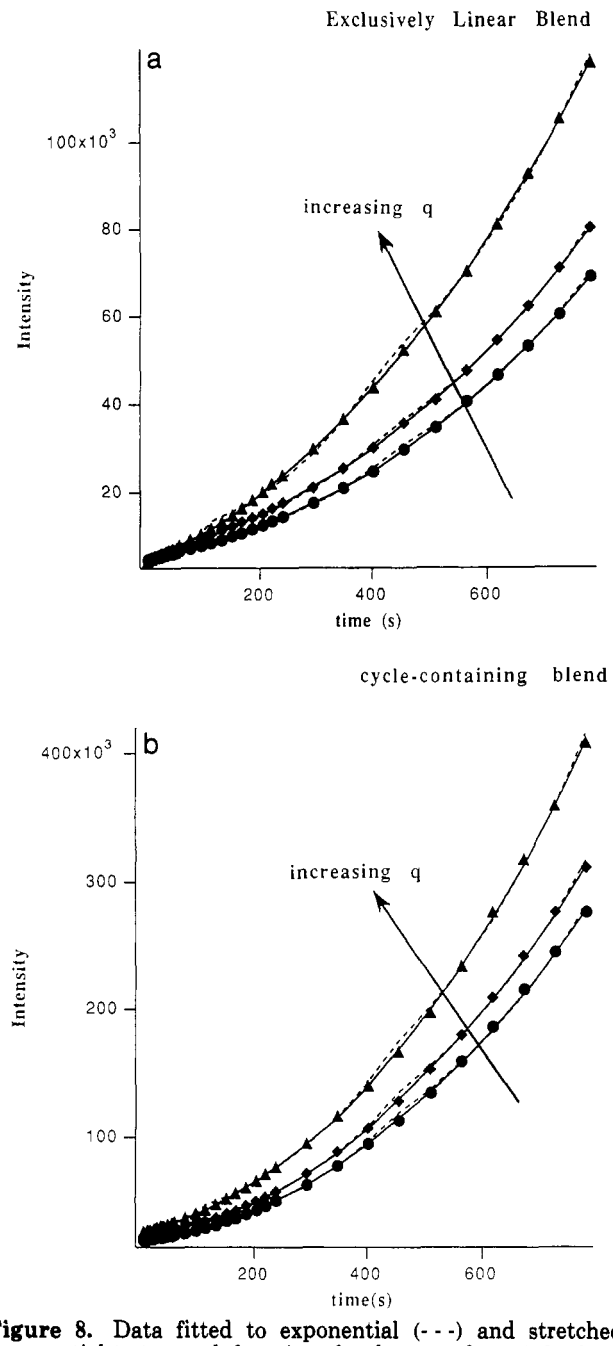

Figure 8. Data fitted to exponential (- - -) and stretched exponential (—) growth functions for three q values: 7.24, 9.46, and 11.49 μm^{-1}: (a) for a blend containing linear PS, temperature = 116 °C; (b) for a blend containing cyclic PS, temperature = 122 °C.

(b) the blend containing cyclic PS. The solid lines represent the fit employing the stretched exponential model in eq A1, while the dashed lines indicate the best fit with eq A2. In both cases, the fits over the full time range of 0–800 s were poor, so in Figure 8, the fit is broken into three time frames (0–300 s, 300–500 s, 500–800 s) each with their own set of parameters and mean square errors.

Figure 8 does not show clearly the superiority of eq A1 to eq A2. Tables AI and AII summarize the parameters and χ^2 values for Figure 8 and also include values for a fit involving the full range from 0 to 800 s. In all cases, the χ^2 values are lower for the stretched exponential analysis than for the purely exponential fit; however, this is to be expected since the former model contains the additional α parameter. Though these tables show only a small subset, they are representative of all our data analysis.

A more interesting feature of our analysis is the evolution of α with the arbitrary time frame. It appears that α decreases as longer times are considered, suggesting greater deviation from linear spinodal decomposition kinetics with increased time, not an earth-shattering result. Further, α decreases with increased q when comparisons are made within the same time frame. This is also consistent with the fact that the maximum in the scattering function moves in from large to small q as time is increased. Because α depends strongly on both q and time, we do not feel that it adds to our physical understanding of the phase separation process; it merely complicates the analysis.

Temperature also affects the calculated value of α for a given time frame, with an increased temperature increment above the spinodal temperature yielding lower α values. This is also consistent with the fact that temperature jumps further into the two-phase region result in more rapid phase separation kinetics such that deviations from the early stage model set in sooner. All the dependencies of α (on q and T, but more importantly on time, even for short times) seem independent of the molecular architecture within the blend, suggesting that no striking difference exists in the mechanism for phase separation.

References and Notes

(1) Klein, J. *Macromolecules* **1986**, *19*, 105.
(2) Roovers, J.; Toporowski, P. M. *Macromolecules* **1983**, *16*, 843.
(3) Roovers, J. *Macromolecules* **1985**, *18*, 1359. Roovers, J. *Macromolecules* **1988**, *21*, 1517.
(4) McKenna, G. B.; Hadziiannou, G.; Lutz, P.; Strazielle, C.; Rempp, P.; Kovacs, A. J. *Macromolecules* **1987**, *20*, 498.
(5) McKenna, G. B.; Hotstetter, B. J.; Hadjichristidis, M.; Fetters, L. J.; Plazek, D. *Macromolecules* **1989**, *22*, 1834.
(6) McKenna, G. B.; Plazek, D. *Polym. Commun.* **1986**, *27*, 304.
(7) Mills, P. J.; Mayer, J. W.; Kramer, E. J.; Hadziiaonnou, G.; Lutz, P.; Strazielle, C.; Rempp, P.; Kovacs, A. J. *Macromolecules* **1987**, *20*, 513.
(8) Flory, P. *Principles of Polymer Chemistry*; Cornell University Press: Ithica, 1953.
(9) Han, C. C.; Bauer, B. J.; Clark, J. C.; Muroga, Y.; Matsushita, Y.; Okada, M.; Tran-Cong, Q.; Chang, T.; Sanchez, I. C. *Polymer* **1988**, *29*, 2002.
(10) Han, C. C.; Okada, M.; Muroga, Y.; McCrackin, F. L.; Bauer, B. J.; Tran-Cong, Q. *Polm. Eng. Sci.* **1986**, *25*, 3.
(11) Hashimoto, T.; Itakura, M.; Shimidzu, M. *J. Chem. Phys.* **1986**, *85*, 6773.
(12) Roovers, J. Personal communication.
(13) Hild, G.; Strazielle, C.; Rempp, P. *Eur. Polym. J.* **1983**, *19*, 721.
(14) Sato, T.; Han, C. C. *J. Chem. Phys.* **1988**, *88*, 2057.
(15) Cates, M. E.; Deutch, J. M. *J. Phys.* **1986**, *47*, 2121.
(16) Pakula, T.; Guyler, S. *Macromolelcules* **1988**, *21*, 1655; *Makromol. Chem.*, in press.
(17) Doi, M.; Edwards, S. F. *The Theory of Polymer Dynamics*; Clarendon Press: Oxford, 1986.
(18) Hadziiannou, G.; Cotts, P. M.; ten Brinke, G.; Han, C. C.; Lutz, P.; Strazielle, C.; Rempp, P.; Kovacs, A. J. *Macromolecules* **1987**, *20*, 493.
(19) Stephenson, G. B. *J. Non-Cryst. Solids* **1984**, *66*, 393.
(20) Di Marzio, E.; Guttman, C. *Macromolecules* **1987**, *20*, 1403.
(21) Certain commercial materials and equipment are identified in this paper in order to adequately specify the experimental procedures. In no case does such identification imply recommendation or endorsement by the National Institute of Standards and Technology, nor does it imply necessarily the best available for the purpose.

Registry No. PS (homopolymer), 9003-53-6; PVME (homopolymer), 9003-09-2.